YUMSUK
JOURNAL OF PURE AND APPLIED SCIENCES

BIO-REMEDIATION OF DYE CONTAINING WASTEWATER USING WATERMELON (*Citrullus lanatus*) RIND AS AN ADSORBENT

[1]Ahmed A., [2]Abdulsalam B.,

Chemistry Department, School of Secondary Education, Sciences, Federal College of Education, Katsina, Nigeria
*Corresponding Author e-mail: ali.ahmedgumel2011@gmail.com Mobile: 08069262755

ABSTRACT

Dyes contaminated wastewaters are commonly discharged as effluents from chemical, textile, leather, plastics and other food industries leading to environmental pollution. Therefore, such challenges need to be scientifically or technologically addressed. Previous remediation approaches have several limitations that may lead to a secondary pollution. Thus, it is recommended to use an eco-friendly and inexpensive approach for wastewater treatment. In this study, the adsorption of Congo Red (CR) and Rhodamine B (RB) dyes from aqueous solution using watermelon (Citrullus lanatus) rind as an adsorbent were modeled. The influence of initial pH, solution temperature, adsorbent and adsorbate concentrations on their percentage removal was studied using batch approach. At initial pH 2, initial concentration of 10 mg/L and 0.5g adsorbent dosage, a significant percentage adsorption removal of about 93% and 98% for Congo Red and Rhodamine B dyes were recorded based on the results of the adsorption experiment. Characterization of the adsorbent was achieved through Fourier Transform Infrared Spectroscopy analysis (FTIR), scanning electron microscopy (SEM) and potential of zero charge determination. Surface characterization of the adsorbent revealed that, upon adsorption, the cloudy and flaky nature of the watermelon rind (WR) tend to disappeared leading to higher surface area for adsorption as ascertained by the potential of zero charge pH based measurements. The fitting experimental data to different conventional kinetic models such as pseudo-first and pseudo second order, Elovich and intraparticle diffusion kinetic models showed that adsorption followed the second-order equation in addition to intraparticle diffusion as the rate-limiting factor. Various adsorption isotherm models, such as Langmuir, Harkins-Jura and Temkin, were applied to the collected experimental data in order to determine the mechanism of Congo red and Rhodamine B dyes adsorption onto watermelon rind (WR). Among the three models tested, Langmuir gave the best fit with highest correlation coefficients (R^2 = 0.999 for Congo Red and R^2 = 1 for Rhodamine B). The work suggests that, watermelon rind (WR) may be utilized as a low cost adsorbent for Congo Red (CR) and Rhodamine B (RB) removal from aqueous solution.

Keywords: Dye, Watermelon Rind (WR), Congo Red (CR), Rhodamine B (RB), Adsorption,

INTRODUCTION

In Nigeria, most of the water used for domestic, agricultural and industrial purposes is channeled from rivers and ground water. The quality of these water bodies cannot be guaranteed due to constant disposal of textile industrial effluents (*Abdulmumini et. al*., 2015). Textile industries are the major consumers of water and produce large volumes of coloured wastewater as byproduct of dyeing and finishing processes. These wastewater often contain high concentrations of synthetic dyes that are recalcitrant, toxic and resistant to conventional biological treatments (Forgacs *et al*., 2023). Conventional wastewater treatment techniques for dye removal, such as chemical oxidation, coagulation, and membrane filtration, can be costly, energy-intensive, and generate secondary waste streams that require further disposal (Gupta and Suhas, 2019).

Recently, adsorption-based methods have gained attention as a sustainable and eco-friendly alternative for the remediation of dye-containing wastewater (Ayat *et al.,* 2023). Adsorbents derived from agricultural waste materials, often called biosorbents, have emerged as promising and efficient adsorbent due to their low cost, availability, and potential for valorization of wastewater. The aim of this study, is to investigate the feasibility of using watermelon rind (WR) for the removal of Congo Red and Rhodamine B dyes with an objectives to characterize the adsorbent, evaluate its adsorption performance, determine the effects of parameters (such as: initial dye concentration, adsorbent dosage, pH and contact time) on the adsorption efficiency as well as investigating the kinetic, isotherm models and thermodynamic parameters.

Ladan *et al.,* (2013), studied batch adsorption assay of Chromium from sediment of river watari. From the results obtained for the adsorption envelop experiments, a good adsorption potential was recorded at initial pH of 2 and a temperature of 25^{o}C and Langmuir isotherm model gave the best fit with regression values ranging from 0.6494 to 0.7459 for 25^{o}C, 30^{o}C, 40^{o}C and 50^{o}C respectively which suggests a homogeneous surface for the sediment.

Sabrine *et al.,* (2023), investigated the adsorption efficiency of new carbon/CNT composites for the removal of cationic dye, Rhodamine B (RhB), from dye-contaminated wastewater. The presence of the carbon nanotubes provided more active sites for dye removal and improved the adsorption behavior of Rhodamine B dye. The applicability of the pseudo-second-order equation could be explained assuming that the overall adsorption rate is limited by the rate of adsorbate transport that occurs on the pore surfaces of adsorbents. Furthermore, the intraparticle diffusion and Bangham models were used to investigate the diffusion mechanism of RhB absorption onto carbon composites which showed multiple adsorption stages occurred simultaneously via pore surface diffusion.

The Dyes selected for the purpose of this research were Congo Red (CR) and Rhodamine B (RB). These dyes have been used extensively used for textile and food dyeing industries; they are very toxic even in lower concentration.

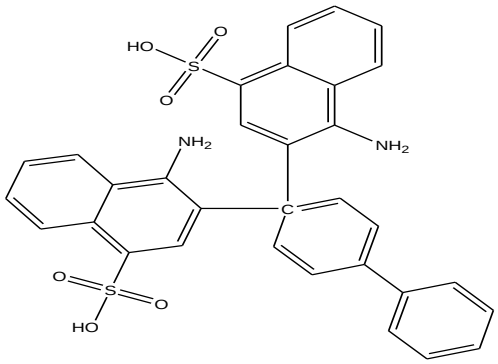

Figure 1(a): Structure of Congo Red (CR) dye

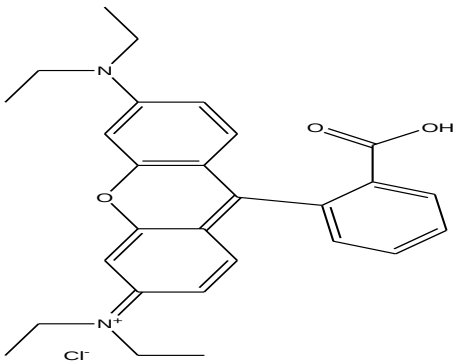

Figure 1(b): Structure of Rhodamine B (RB) dye

MATERIALS AND METHOD

The materials used include routine laboratory glass wares; weighing balance (FA2004 Electronic Balance, NO: SHP02004413 2011-06), UV-Vis spectrometer (Cary 50, version 3.0), Fourier transform infrared spectroscopy (Cary 630; Agilent Technologies), Scanning Electron Microscope (SEM, Leica Stereoscan-440 interfaced with Phoenix EDX, Furnance (LF3 from V. Ltd) and pH Meter (JENWAY, 3510).

Analytical grade reagents were; $CuCl_2.2H_2O$, Congo

Red (C.I:22120, Loba Chemie),Rhodamine B ((98.5% Sigma Aldrich)),NaOH (JDH, 99%) HCl (Sigma Aldrich, 37, sp.gr.1.18gcm^3), H_2SO_4 (Sigma Aldrich, 98% pure, sp.gr. 1.84 gcm^3)

2.1 Preparation of Watermelon rind (Adsorbent)

The watermelon rind wastes were cut into small pieces and sun dried. The rinds wastes were completely mixed with concentrated sulphuric acid in the ratio 1:1 and Placed in a Muffle furnace (LF3 from V. Ltd.) at 300^{o}C for 3 hours. The sample was then removed, cooled and washed with distilled water till the pH reaches 7. The sample was then made powdered and further oven dried at 105^{o}C to constant weight and stored.

Figure 2: Prepared Watermelon Rind

2.2 Adsorbent Characterizations

2.2.1 Scanning Electron Microscopic (SEM) Analysis

The SEM analyses were performed for both spent and unused adsorbent samples using Leica Stereo 440 model SEM Machine at Umar Musa Yar' Adua University, Katsina to acquire information on porosity and cavities on the surface of the adsorbent before and after adsorption. It was also aimed at knowing whether pore-diffusion adsorption took place.

2.2.2 FT-IR Analysis

Fourier transform infrared spectrometer (Carry 630) Agilent Technologies was used for FTIR spectral analyses in the wave number range of 4000 - 650cm^{-1}. The analyses were carried out at the Department of Pure and Industrial Chemistry Bayero University Kano, before and after biosorption, to establish whether the functional groups present are responsible for the biosorption.

2.2.3 pH at Point of zero charge (pH_{pzc})

The zero surface charge (pH_{pzc}) characteristics of the adsorbents was determined, using the solid addition method before and after adsorption. 40 cm^3 of 0.1M NaCl solution was transferred to a series of 100cm^3 stoppered conical flasks. The pH_i values of the solutions were adjusted between 2 to 11 by adding either 0.1M HCl or 0.1M NaOH.

2.3 Preparation of Adsorbates

The anionic dye (CR) and cationic dye (RB) were purchased from Sigma-Aldrich. The chemical structures of CR and RB are shown in Figure 1. The CR and RB stock solutions of 1.0 g L^{-1} concentration were prepared, and the desired experimental concentrations were made up by diluting the stock solution with distilled water. The pH of solutions was adjusted using 0.1 M HCl and 0.1 M NaOH solutions.

2.4 Batch Adsorption Studies

Adsorption study of CR and RB dyes was performed using WMR as the adsorbent. The batch experiments were conducted using a known quantity of adsorbent and a volume of 100 mL of dye solution at a known initial concentration in an Erlenmeyer flask. The flask was placed in a shaker at 300 rpm at 25℃. The samples were examined at certain time intervals, and the solutions were filtered using Whatman No. 41 filter paper and centrifuged at 2000rpm for 15 minutes. The concentrations of samples was analyzed using UV-visible double-beam spectrophotometer (UV-6100 PC, China). The effect of adsorbent dose (0.1 – 0.5g), reaction time (5-120 min.), initial dye concentration (10-310mg/L), pH (2-12) and temperature (303-318K) were evaluated. The adsorption capacity, qe (mg g^{-1}), and the adsorption efficiency, R (percent of adsorbate adsorbed), were calculated using Equations (1) and (2):

$$q_e = \frac{(C_i - C_e)}{mAWR} \times V \quad \text{.....(1)}$$

The equation (1) above, can be express in terms of % removal as:

$$R = \frac{(C_i - C_e)}{C_i} x100\% \quad \text{.....(2)}$$

Where C_i and C_e are the initial concentration and equilibrium concentration of the CR and RB solutions (mg L^{-1}), respectively, mWR is the mass of adsorbent (g), and V (L) is the volume of the solution. The amount of dye adsorbed at any time, q_e (mg g^{-1}), was calculated using Equation (3):

$$q_t = \frac{(C_i - C_t)}{mAWR} \times V \quad \text{..... (3)}$$

Where C_t (mg L^{-1}) is the dye concentration at time t.

2.5 Adsorption Thermodynamic

The thermodynamic parameters Gibbs free energy (ΔG), enthalpy (ΔH), and entropy (ΔS) are given by the following equations:

$$\Delta G = -RTln\,(K_d) \quad \text{..... (4)}$$

$$\Delta G = \Delta H - T\Delta S \quad \text{..... (5)}$$

Where R is the universal gas constant (8.314 $Jmol^{-1}K^{-1}$), T is absolute temperature in Kelvin (K) and K_d is the apparent adsorption equilibrium constant, and can be determined as follows:

$$K_d = \frac{q_e}{C_e} \quad \text{..... (6)}$$

ΔH and ΔS were computed from adsorption data at different temperatures using the Van't Hoff Equation:

$$ln(K_d) = \frac{1}{R}\left(\frac{\Delta S - \Delta H}{T}\right) \quad \text{..... (7)}$$

2.6 Isotherms and Kinetic Studies

Studying the adsorption isotherm data is important to investigate the interaction between the adsorbent and the adsorbate, and it is necessary to understand the adsorption mechanisms.

Adsorption isotherms of CR and RB Dyes by WMR was evaluated using batch equilibrium assays. Effects of initial pH, adsorbent (WR) dosage, adsorbate (dyes) dosage, temperature and possibly contact time were taken into considerations (Ladan *et al.*,2013).

Three isotherm models (Harkins-Jura, Langmuir and Temkin) were used to study the behavior of CR and RB adsorption on the W.

Table 1: **Equations and parameters of isotherm and kinetics**

Model	Name	Nonlinear	Linear equation	Parameters
	Temkin	$q_e = q_m \ln(K_T\, C_e)$	$q_e = q_m \ln K_T + q_m \ln C_e$	Ce: Concentration of dye at equilibrium $mg\ L^{-1}$)
Isotherm	Freundlich	$q_e = k_f c_e \frac{1}{n}$	$\ln = \ln k_f + \frac{1}{n} \ln c_e$	qe: Amount of adsorbate adsorbed per unit $K_T = temkin\ constant$
	Harkins-Jura	$q_e = \left(\frac{A_H}{B_H - log C_e}\right)^{1/2}$	$\frac{1}{{q_e}^2} = \frac{BH_J}{AH_J} - \frac{log C_e}{AH_J}$	mass of adsorbent at equilibrium $mg\ g^{-1}$)
	Pseudo-first order	$q_t = q_e\left(1 - exp^{-k_{1pt}}\right)$	$\ln(q_e - q_t) = \ln q_e - k_{1pt}$	q_t: $adsorbate\ adsorbed\ at\ time\ t(mg\ g$
	Second order	$q_t = \frac{q_e}{(1+k_{2qet})}$	$\frac{1}{q_t} = \frac{1}{q_e} + k_2 t$	k_{1p} = pseudo first order rate constant
Kinetics	Pseudo-second order	$q_t = \frac{k_{2pq_e{}^2t}}{1+k_{2pq_e t}}$	$\frac{1}{q_t} = \frac{1}{k_{2pq_e{}^2t}} + \frac{t}{q_e}$	k_{2p} = pseudo second order rate constant
	Intraparticle diffusion	$q_e = k_{int}\, t^{1/2}$		k_{int} = intraparticle diffusion rate constant

RESULT AND DISCUSSION

3.1 Characterization of WR

3.1.1 Fourier Transform Infrared Spectroscopy (FT-IR)

The pattern of adsorption onto WMR biomaterial is highly associated with the availability of the active functional groups and bonds of the WR surface. For the elucidation of these active sites, FTIR spectroscopy was performed onto the raw watermelon rind (WR) in the range (4000–1000 cm^{-1}) as shown in figure 3.

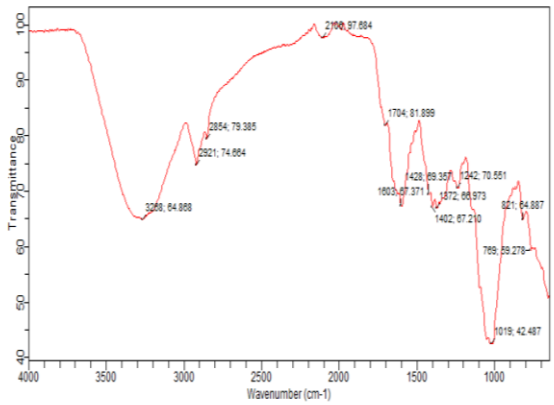

Figure 3: FTIR spectra of raw watermelon rind (WR) before adsorption

The FTIR spectrum of the raw rind showed that, oxygen (51.50 wt. %) and carbon (41.50 wt. %) are the major constituents of WR along with the quantifiable amount of hydrogen (6.12 wt. %) and nitrogen (0.88 wt. %) which can interact with the dye molecule via an electrostatic interactions (Ali *et al.*, 2023).

Figure 4, depicted the FTIR spectrum of watermelon rind after the adsorption of Congo Red dye. The broad and intense band at 3268 cm^{-1} is attributed by the –OH stretching vibrations of cellulose, pectin and lignin while the band at 2922 cm^{-1} corresponds to the –CH stretching vibrations of the methyl group. The band at 1735 cm^{-1} indicates the C=O stretching of carboxylic acid or esters.

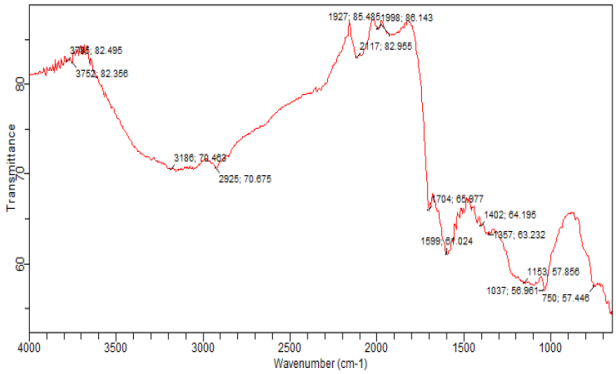

Figure 4: FT-IR Spectrum of watermelon rind after Adsorption of Congo Red Dye.

However, the asymmetric and symmetric vibrations of –COO of the ionic carboxylic groups within WMR are represented by the band at 1630 and 1433 cm^{-1}, respectively. The band at 1380 cm^{-1} can be ascribed to the symmetric stretching of –COO of pectin.

The spectrum of watermelon rind after the adsorption of Rhodamine B dye was showed in figure 5. The IR bands between the 1300 and 1000 cm−1 region are assigned to the C–O and C–O–C stretching vibrations in carboxylic acids, alcohols, phenols or ester groups.

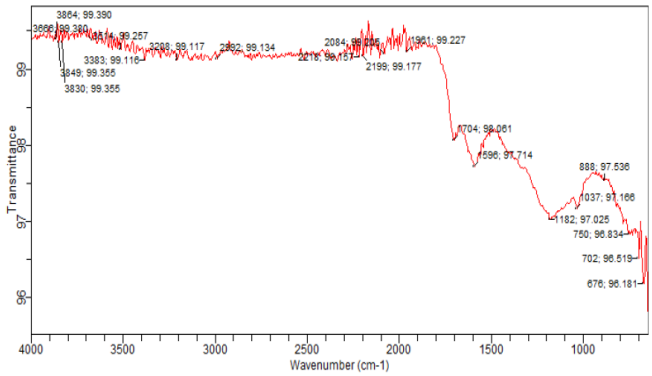

Figure 5: FT-IR Spectrum of watermelon rind after the Adsorption of Rhodamine B Dye.

FTIR spectrum of raw WR is rich in carboxylic and hydroxyl groups, which can be deprotonated to bind the positively charged Rhodamine B. This assertion agrees with result reported by Manal *et al.*, (2012).

3.1.2 Scanning Electron Microscopic (SEM) Analysis of the Adsorbent

SEM analysis was employed to study the surface morphology of WMR before and after the adsorption of CR and RB. Figure 5 shows the

SEM image of the raw watermelon rind (WMR); several pores with varied sizes were observed on the surface of the WMR. Figure 6 and 7 display the aggregation of CR and RB, respectively, on the surface of WMR.

From Figure 4, the WMR before RB adsorption possesses uneven and irregular surface with considerable layers of rough heterogeneous pores which offers high possibility for dye molecules to be adsorbed (Hameed, 2018). Thus, the SEM image of WMR after the dyes adsorption in Figure 6 and 7 reveal smoother surface features with apparent reduced pore structures, indicating the uptake and entrapment of RB molecules by the accessible pore vicinities of the WMR surface, which proves the engagement of CR and RB adsorption onto WMR and this may be related to the presence of carboxylic and hydroxyl groups within WMR, as evidenced by the IR spectral (Figure 3), which act as active sites for the adsorption of dye molecules.

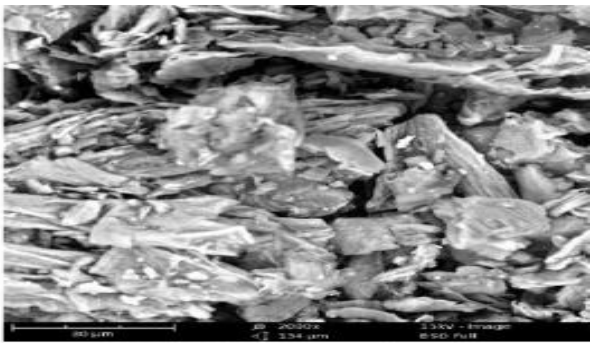

Figure 5: SEM Image of Watermelon Rind (WR).

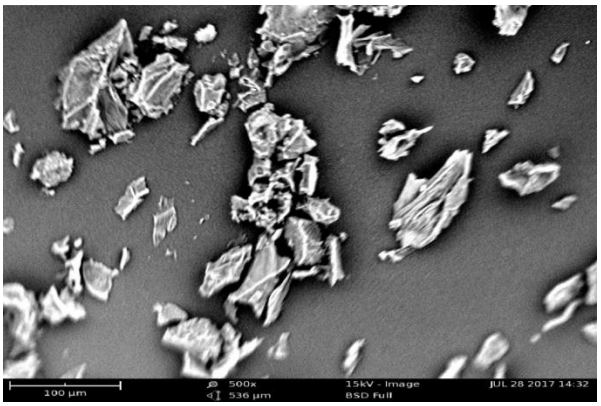

Figure 6: SEM Image of the adsorbent after Adsorption of CR

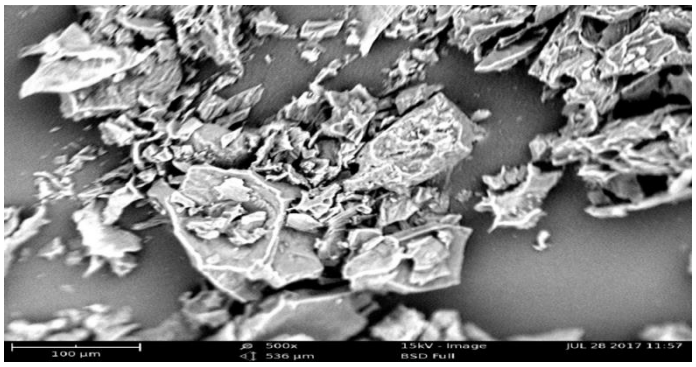

Figure 7: SEM Image of Watermelon Rind (WR) after Adsorption of Rhodamine B.

3.1.3 pH at Point of zero Charge (pH_{pzc})

The pHpzc of WMR was determined to find out the pH at which the electrical charge of the surface of WMR was zero. Figure 8 shows that the pHpzc of WMR was at pH 2.0 which reflected the acidity of WMR, in agreement with the aforementioned IR results (Figure 5) that carboxylic acids are present in abundance within WMR. Adsorption of anionic dye (CR) is favoured at solution pH below the pHpzc value as the surface of WMR is positively charged due to protonation whereas at solution pH above the pHpzc value, the surface of WMR becomes negatively charged and thus, adsorption of cationic dye (RB) is preferred. In this regard, it is predicted that the adsorption of the cationic RB by WMR will be appropriate at solution pH above 2.0 because of electrostatic interactions (Lopez *et al.*, 2008).

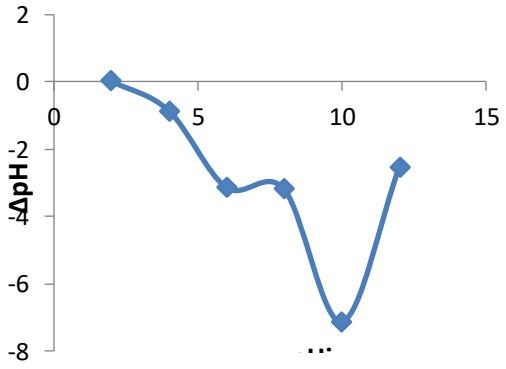

Figure 8: pHzpc of WMR Suspensions

3.2 Batch mode adsorption of CR and RB

3.2.1 Effect of contact time

The contact time was investigated up to 120 min,

as displayed in Figure 9, with a dye concentration of 100 mgL^{-1}, a temperature of 25 ^0C, and WMR dose of 0.3 mgL^{-1}. The adsorption of both dyes is increased with increasing time until it reaches equilibrium after 60 min for CR, with 92% removal, and 30 min for RB, with 98% removal.

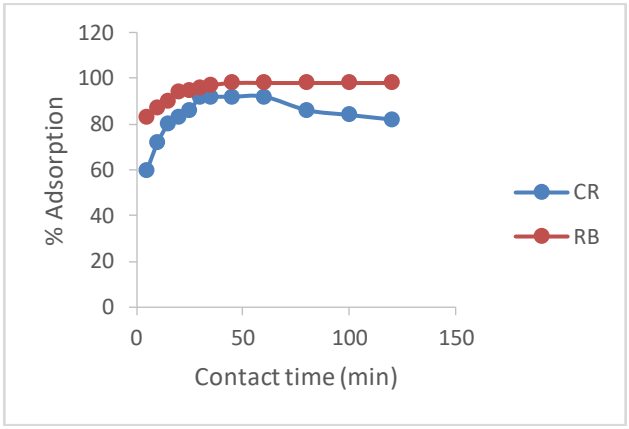

Figure 9: Effect of contact time

3.2.2 Effect of Adsorbent dosage

The WMR dose was investigated in the range of 0.1–0.5g for CR and RB Dye molecules. The effect of adsorbent dose on percentage removal 96 to~100% for RB and 55 to 94 for Congo red was depicted in figure 10 respectively, as the dose of the adsorbent increased from 0.1 to 0.5g. The percent removal increased with an increase in sorbent dose which might be due to an increase in the number of sorption site available for adsorption. This agreed with the result previously reported by (Zaharraddeen *et al.*, 2015, Wong *et al.*, 2009).

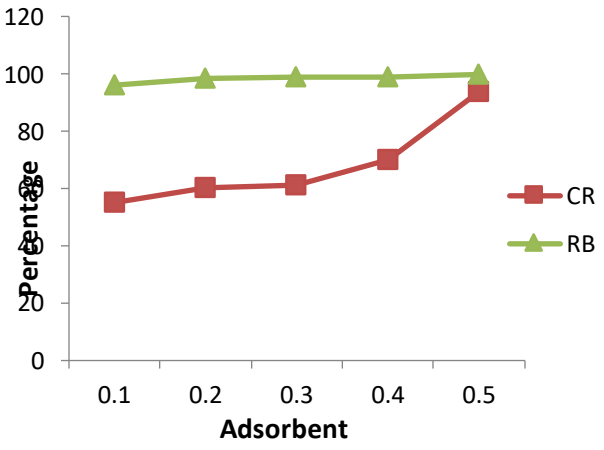

Figure 10: Effect of Adsorbent Dosage

3.2.3 The effect of initial dye concentration

The effect of initial dye concentrations was examined in the range of 10–130 mg L^{-1} for the dyes (masswmr = 0.5 g). As Figure 11 shows, the removal efficiency of both dyes is decreased as the initial concentration of the dyes increases, and this may be attributed to the limited number of adsorption sites that are present on the WR surface (Monsour *et al.*, 2021).

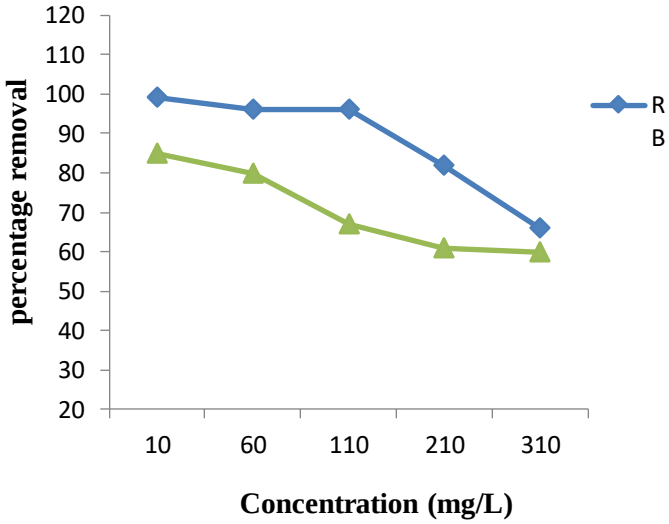

Figure 11: Effect of Concentration

3.2.4 Effect of Temperature

The effect of adsorption temperature was examined at a temperature of 303, 308 and 313^0C for 100 mg L^{-1} of the CR and RB dyes, as shown in Figure 12. The percentage removal of both dyes increases as the adsorption temperature increases. The results indicate the endothermic nature of the adsorption reaction for both dyes onto WMR surface.

Figure 12: Percentage adsorption as a function of the Temperature.

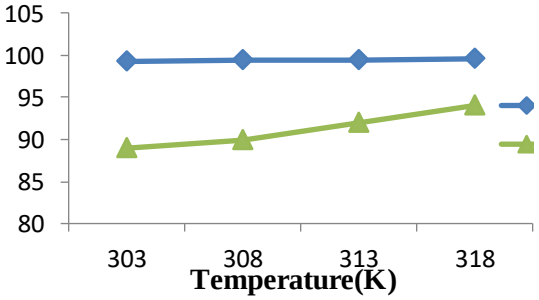

Table 2: Isotherm Models

Dye	Harkins-Jura			Freundlich isotherm			Temkin Isotherm		
	AH_J	BH_J	R^2	K_f	n	R^2	K_T	B_1	R^2
CR	-98.04	-1.962	0.98	5.33	3.7	0.99	0.66	21.1	0.93
RB	153	0.6	0.999	3.85	2.56	0.987	-0.03	0.06	0.99

4.0 Result and Discussion

4.1 Isotherm Models, Kinetics and Thermodynamics Adsorption studies

The isotherm, kinetics and thermodynamic adsorption studies for CR and RB dyes onto WMR results were depicted in table 1 above.

Freundlich, Temkin and Harkins-Jura isotherm were modeled in this work as shown in table 2. The Harkin-Jura model stands fit for both dyes, With maximum R^2 for RB (R^2 = 0.999) and CR (R^2 = 0.989). Additionally, the k_f value of CR (3.7) was larger than that of RB (2.5), demonstrating that WMR has greater adsorption energy with CR than RB (Djilina *et al.*, 2015). In the Freundlich model, the values of 1/n were 0.270 for CR and 0.390 for RB; this suggested favorable adsorption of both dyes ($0.1 < \frac{1}{n} < 1$) at WMR. The smallest values for R^2 for both dyes were calculated using the Temkin model.

Table 3: Adsorption Kinetic Parameters of CR and RB Dyes.

Parameter	Congo Red (CR) DYE	Rhodamine B (RB)
Pseudo First order (min^{-1})	k_1 = 0.0165 R^2 (0.4835)	k_1 (0.0235) R^2 (0.1756)
Pseudo Second order($mg.g^{-1}min^{-1}$)	k_2 = 0.04745 R^2 (0.9996)	k_2 (0.015) R^2 (1)
Second Order ($mg.g^{-1}min^{-1}$)	k_2 =0.0009 R^2 (0.3787)	k_2 (-0.0000) R^2 (0.4210)
Intraparticle diffusion (mg g^{-1} $min^{-1)}$	K_{diff} **(0.3) C(0.63)** R^2**(0.97)**	K_{diff} **(0.12) C(8.59)** R^2**(0.59)**

Pseudo-first order, second order, pseudo-second order, and intraparticle diffusion kinetic models were employed in this study (as shown above in table 3). The obtained parameters for these models are listed in Table 3. Based on the highest correlation coefficient values, the adsorption of both anionic CR (R^2 = 0.9917), and cationic RB(R^2 = 1) dyes follow the pseudo-second order kinetic model, similar work was reported by manal *et al.*,(2023). Due to the nonzero intercept, the interaparticle diffusion model did not fit with the experimental data for both dyes.

Table 4: Adsorption Thermodynamics Parameters of CR and RB Dyes

Dyes	Temperature (K)	ΔG (J/mol)	ΔH (J/mol)	ΔS ($Jmol^{-1}K^{-1}$)
CR	303	-90		
	308	-132	2449	8.38
	313	-176		
RB	303	-206.6		
	308	-210.6	158.9	12.4
	313	-216.6		

The values of ΔH and ΔS were determined based on the slope and the intercept from the plot of ln (K_d) vs. 1/T. The values of ΔG were calculated at different temperatures according to Equation (5). The values of ΔH, ΔS and ΔG are presented in Table 4. Corresponding to the results, all values of ΔG were negative for CR and RB adsorption, indicating that the adsorption process is spontaneous for both. The positive values of ΔH indicate that, the sorption process is endothermic. Moreover, positive values of ΔS (CR: 8.38 $Jmol^{-1}K^{-1}$; 10.8 $Jmol^{-1}K^{-1}$; RB: 12.4 $Jmol^{-1}K^{-1}$) values showed the increase in the affinity of the dyes onto adsorbent and also suggested the increased randomness at the solid-solution interface during the adsorption process. The dye molecules in the aqueous media are hydrated. When the dye molecule get adsorbed onto the adsorbent surface, the water molecules previously hydrogen bonded to the dye molecule get released and dispersed in the solution, this results in an increase in the entropy. The positive values of the ΔS reflected good affinity of the dyes toward the adsorbent. This result was in excellent agreement with literatures (Xunjun, 2015, Yamunadevi *et al.,* 2016; Ali *et al.,* 2017

CONCLUSION

Watermelon rind (WMR), was effectively utilized for the adsorption of anionic Congo red dye and the cationic Rhodamine B dyefrom an aqueous solution. The findings obtained for CR and RB adsorption onto WMR show that the percentage removal of cationic dye is better than that of anionic dye. The Harkin-Jura model indicated the best fit for both dyes, with maximum R^2 for RB (R^2 = 0.999) and CR (R^2 = 0.989). The adsorption kinetics of was well fitted using second order model, respectively. The equilibrium removal of the dyes increased as the temperature of solution increases, because the adsorption was chemical. The adsorption processes of CR and RB by WMR were endothermic and spontaneous.

REFERENCES

Abdulmumini, Ado, Abubakar, I., Magaji, L., Sani, M., Ayuba A. M., Shehu, H., & Isa B.(2023). A Review on Industrial Effluents as Major Sources of Water Pollution in Nigeria. Journal of American Institute of science, **1**(5),159-164.

Alberto, U., Paul L.B. and Neville G.P. (2002), 'The influence of pH and temperature changes on the adsorption behavior of organophilic clays used in the stabilization/solidification of hazardous wastes', Journal of Environmental Engineering Sciences, **1**(1), 123-133.

Ali, H., Jawad, Y., Ngoh, S., & Khairul A.(2018). Utilization of watermelon (Citrullus lanatus) rinds as a natural low-cost biosorbent for adsorption of methylene blue: kinetic, equilibrium and thermodynamic studies. Journal of Taibah University for Science, DOI:10.1080/16583655.2018.1476206.

Aseel, M,. Abbas, N., Alshirifi A., & Ayad, F.(2014).Kinetics and equilibrium study for the adsorption of textile dyes on coconut shell activated carbon. Arabian Journal of Chemistry. https://doi.org/10.1016/j.arabjc.2014.o1.020.

Ayat, T.,Walaa, H., & Shaymaa, A.(2023). Bioremediation of Heavy Metals in Wastewaters: A Concise Review. Egyptian Journal of Aquatic Biology & Fisheries, **27**(1), 143 – 166.

Cameselle C, Gouveia S, Akretche DE, Belhadj B (2013) Advances in electrokinetic remediation for the removal of organic contaminants in soil. In: Rashed MN (ed.), Soils, Organic Pollutants-Monitoring, Risk and Treatment.

Dabrowski, A. (2001). Adsorption from Theory to Practice, Advances in Colloid and Interface Science, (93), 135-224.

Hameed BH., & El-Khaiary MI. (2018).Removal of basic dye from aqueous medium using a novel agricultural waste material pumpkin seed hull. International Conference on Agriculture, Environment and Biological Sciences **155**(3), 601–609.

Jingxi, T. Xiaohong, F. Xiaolei, W.,Yao, Z. Tian, G. Shujun, D. Guoting, L. and Dengyong, T.(2017). Adsorptive Removal of a Reactive Azo Dye Using Polyaniline-Intercalated Bentonite, Pollution. Journal for Environmental Study, DOI: 10.15244/pjoes/67554.

Ladan, M., Ayuba, A. M., Bishir, U., Jamilu, A. & Habibu, S.(2013).Thermodynamic Properties of Chromium Adsorption by Sediments of River Watari, Kano State. ChemSearch Journal **4**(1): 1 – 5.

Litefti, K., Freire, M.S., Stitou, M. & González,Á. J. (2019). Adsorption of an Anionic Dye (Congo Red) from Aqueous Solutions by Pine Bark. Scientific Report Journal 160-530.

Lopez-Ramon, M.V., Stoeckli, F., & Moreno, C.(2008). On the characterization of acidic and basic surface sites on carbons by various techniques Carbon. South African Journal of Chemical Engineering **3**(7), 1215–1221.

Manal, A., Alaa, M., Gada, E., Tasneem, S., & Heba, A.(2023).Adsorption of Anionic and Cationic Dyes on Activated Carbon Prepared from Oak Cupules: Kinetics and Thermodynamics Studies.International Journal of Environmental Research and Public Health. https://doi.org/10.3390/ijerph20043280

Mater, H., Mahnashi I., Samer S., Abu-A., Mohammad, W., & Ali, O.(2021). Kinetics and thermodynamics of enhanced adsorption of E120 dye using activated carbon.Tropical Journal of Pharmaceutical Research, **20** (3), 585-592. http://dx.do oi.org/10.4314/tjpr.

Monina, Sabio M. and Rodriguez Rinoso F.

(2004), 'Role of chemical activation in the development of carbon porosity', Colloids and Surfaces A: Physicochem. Eng. Aspects, (241),15-25.

Patrick B., Godfred O., Lawrence D., Yen A., Eugene A., Sampson O., Barnabas A.(2023). Waste Biomass and Biomaterials Adsorbents for Wastewater Treatment. Green Energy and Environmental Technology, **21**(2), 1–25. https://doi.org/10.5772/.

Sabrine, Z., Ilyes, J.,Marc, C.,Sophie, C., & Makki, A.(2023). Adsorptive Removal of Rhodamine B Dye Using Carbon Graphite/CNT Composites as Adsorbents: Kinetics, Isotherms and Thermodynamic Study. Multidisciplinary Digital Publishing Institute(MDPI). https://doi.org/10.3390/ma16031015.

Ta, W. S., and Chi, K. L., (2016), Removal of Dye by Adsorption: A Review. International Journalof American Educational Research, **11**(4), 2675-2679.

Wahid A., Hamood A., Norzila O.,, Adel Al., Nur H., Mohd D.,Syazwani M.(2023). Adsorption of Zn^{2+} from Synthetic Wastewater Using Dried Watermelon Rind (D-WMR): An Overview of Nonlinear and Linear Regression and Error Analysis.Multidisciplinary Digital Publishing Institute(MDPI). https://doi.org/10.3390/

Wei, L., Bingnan, M. & Yiqi, Y. (2023). Feasibility of industrial-scale treatment of dye wastewater via bioadsorption technology.https://www.sciencedirect.com/sci/pii/so96085.

Xunjun, C.(2015). Modeling of Experimental Adsorption Isotherm Data. Open Access Journal, ISSN 2078-2489. doi:10.3390/info6010014.

Yamunadevi R. Y, Venkatachalam R., Arivoli S and Marimuthu V.(2016), Kinetic, Thermodynamic and Isotherm Studies on the Removal of Rhodamine B Dye using Activated Cyamopsis Tetragonoloba Stem Nano Carbon.Open Access Journal 6(3), 932-943.

Yaneva, Z. & Georgieva, N. (2014). Study on the Physical Chemistry, Equilibrium and Kinetic Mechanism of Azure A Biosorption by Zea Mays Biomass. Journal of Dispersion Sciences and technology **3**(5): 193-204.

Zaharaddeen N. Garba., Zakariyya, U., Zangoa, A. A. Babandob & A. Galadima(2015): Competitive adsorption of dyes onto granular activated carbon. Journal of Chemical and Pharmaceutical Research, **7**(4):710-717.